Structure and Photophysical Properties of an Upconversion Holmium-mercury Compound with a 2-*D* Layer-like Motif ①

CHEN Wen-Tong[a, b, c②]

[a] (*Institute of Applied Chemistry, School of Chemistry and Chemical Engineering, Ji'an Key Laboratory of Photoelectric Crystal Materials and Device, Humic Acid Utilization Engineering Research Center of Jiangxi Province, Jiangxi Province Key Laboratory of Coordination Chemistry, Jinggangshan University, Ji'an* 343009, *China*)

[b] (*Department of Ecological and Resources Engineering, Fujian Key Laboratory of Eco-industrial Green Technology, Wuyi University, Wuyishan* 354300, *China*)

[c] (*State Key Laboratory of Structural Chemistry, Fujian Institute of Research on the Structure of Matter, Chinese Academy of Sciences, Fuzhou* 350002, *China*)

Dedicated to Professor Jin-Shun Huang on the Occasion of His 80th Birthday

ABSTRACT Using a hydrothermal reaction, a novel holmium-mercury compound $\{[Ho(IA)(HIA)_2(H_2O)_2]_2$-$(Hg_3Br_8)\}_n(n HgBr_2)$ $2nNO_3$ (**1**, HIA is isonicotinc acid) was synthesized and its crystal structure was characterized by single-crystal X-ray diffraction. Compound **1** crystallizes in monoclinic system, space group $P2/c$ with a = 13.0647(6), b = 9.4659(3), c = 26.0832(14) Å, β = 97.522(4)°, V = 3197.9(2) Å^3, $C_{36}H_{36}Br_{10}Hg_4Ho_2N_8O_{22}$, M_r = 2863.95, Z = 2, D_c = 2.974 g/cm^3, μ(Mo$K\alpha$) = 18.331 mm^{-1} and F(000) = 2575. It displays a two-dimensional (2D) layer-like structure. A solid-state photoluminescence experiment revealed that it shows upconversion green emission. The emission peaks should come from the $^5I_8 \rightarrow {}^5G_6$ and $^5S_2 \rightarrow {}^5I_8$ characteristic emission of the 4f electrons of the Ho^{3+} ion. Compound **1** has a CIE chromaticity coordinate (0.1774, 0.526). A solid-state UV-visible diffuse reflectance spectrum unveiled that this compound has a wide optical band gap of 3.26 eV.

Keywords: CIE, holmium, lanthanide, photoluminescence, upconversion;

DOI: 10.14102/j.cnki.0254–5861.2011–2762

1 INTRODUCTION

Most of the lanthanide elements (not including La and Lu) show fine photoluminescence performances and, recently, lanthanide materials with photoluminescence performances have drawn more and more attention from chemical, physical and material researchers[1-4]. Nowadays, a large number of researchers are devoting themselves to the design, synthesis, structures, physical and chemical characterization of novel lanthanide materials to investigate the potential and broad applications of lanthanide materials in cell imaging, magnetic materials, catalysts, electrochemical displays, light-emitting diodes, sensors, luminescent probes, and so forth[5-9]. Relative to the broad investigation on the photoluminescence performances of lanthanide materials, there are only few examples of investigation on the semiconductor performances of lanthanide materials and, therefore, more exploration is still necessary[10].

Transition metal materials usually possess attractive properties that enable them to have potential applications in the fields of materials, chemistry, physics, biology, etc. Therefore, transition metal materials have gained more and more attention since many years ago[11-23]. In recent years, a large number of transition metal materials have been documented[24-37]. Amongst the transition metal materials, group 12 (IIB) ones are fascinate due to the following reasons:

Received 10 February 2020; accepted 2 April 2020 (**CCDC 1982611**)

① This project was supported by the NNSFC (21361013), Jiangxi Provincial Department of Education's Item of Science and Technology (GJJ170637) and the Open Foundation of State Key Laboratory of Structural Chemistry (20180008)

② Corresponding author. Professor, majoring in coordination chemistry. E-mails: wtchen_2000@aliyun.com

the vital role of zinc played in biological systems, the broad applications of IIB materials, photoelectric and photo-luminescence behavior, as well as different coordination motifs offered by the d^{10} geometries of IIB cations[38-40]. Mercury is an interesting element and has also gained much attention over the years because of various coordination modes, semiconductor properties, photoluminescence properties, optoelectronic behaviors and so on.

To my knowledge, isonicotinic acid is an important organic molecule. It can be applied as a useful building ligand because it possesses two carboxyl oxygen atoms at one end and one nitrogen atom at the other end. These oxygen and nitrogen atoms enable isonicotinic acid to bind to several metal centers and yield an extended structure with different coordination motifs. It is well-known that oxygen atoms are favorable to bind to lanthanide ions, while nitrogen atoms tend to coordinate to transition metal ions. Therefore, it is deemed that isonicotinic acid can simultaneously coordinate to both lanthanide and transition metal ions. Over the years, the investigation of materials with attractive photoluminescence and semiconductor performances, especially lanthanide mercury materials, have become one of my research topics with a view to getting new findings in crystal structures, photoluminescence and semiconductor performances. In the present paper, the hydrothermal preparation, X-ray structure, photophysical performances and thermogravimetry of a novel holmium-mercury material, $\{[Ho(IA)(HIA)_2(H_2O)_2]_2(Hg_3Br_8)\}_n$ (nHgBr$_2$) 2nNO$_3$ (**1**, HIA is isonicotinc acid), are reported. It is characterized by a 2-*D* layer-like structure. It is noteworthy that this compound exhibits upconversion green emission.

2 EXPERIMENTAL

2. 1 General procedures

In the present work, all chemicals and/or reagents for the preparation of complex **1** were of AR grade purity, commercially bought and used directly without purification. The infrared spectrum was carried out using a PE Spectrum-One FT-IR spectrophotometer with a KBr pellet. The solid-state photoluminescence spectra were carried out with a F97XP photoluminescence spectrometer. A solid-state UV-visible diffuse reflectance spectrum was carried out using a TU1901 UV-visible spectrometer. A powder X-ray diffraction (PXRD) pattern was measured on a AL-Y3000 powder diffractometer with Cu-$K\alpha$ (λ = 1.54056 Å) at a step size of 0.02 °. The simulated powder pattern was obtained by using single-crystal X-ray diffraction data and processed by the free Mercury v1.4 program provided by the Cambridge Crystallographic Data Centre. A thermogravimetry (TG) curve was measured on a NETZSCH TG 209F3 analyzer under nitrogen atmosphere.

2. 2 Synthesis of 1

A mixture of 2.5 mmol $HgBr_2$ (900 mg), 1 mmol $Ho(NO_3)_3$ $6H_2O$ (459 mg), 3 mmol isonicotinic acid (369 mg) and distilled water (10 mL) was put into a stainless-steel Teflon-lined reactor (23 mL) and heated at 160 ℃ for 15 days, then powered off. Colorless prism-like crystals can be obtained once the reactor was cooled down to room temperature and, the crystal was filtered and cleaned with water. The yield of the crystal obtained was 47% based on $Ho(NO_3)_3$ $6H_2O$. IR peaks (cm^{-1}): 3442(vs), 3137(w), 3079(w), 2888(w), 2430(w), 1710(w), 1621(vs), 1500(w), 1411(vs), 1385(vs), 1302(w), 1232(w), 1054(w), 1010(w), 851(w), 768(m), 679(m), 551(w) and 412(m). The purity of the product was confirmed by PXRD, as shown in Fig. 1.

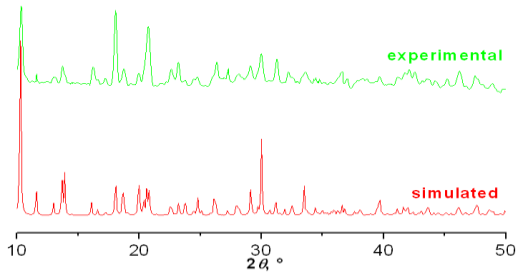

Fig. 1. PXRD pattern of compound 1

2. 3 X-ray structural determination

Using a carefully selected crystal, the single-crystal X-ray diffraction data set of complex **1** was obtained from a SuperNova CCD X-ray diffractometer equipped with a graphite-monochromated Mo$K\alpha$ radiation (λ = 0.71073 Å). The data reduction and empirical absorption were performed with CrystalClear software. By using direct methods, the crystal structure of **1** was resolved with SHELXS software[41] and refined on F^2 with a full-matrix least-square. All of the non-H atoms were found based on the difference Fourier spots and anisotropically refined, while all of the H atoms were theoretically identified, attached to the parent atoms and isotropically refined. Reflections collected are 17376; the final R = 0.0874 for 381 parameters and 3310 observed reflections with $I > 2\sigma(I)$ and wR = 0.2233 ($w = 1/[\sigma^2(F_o^2) + (0.1212P)^2 + 30.1388P]$, where $P = (F_o^2 + 2F_c^2)/3$); S = 1.078, $(\Delta\rho)_{max}$ = 3.874, $(\Delta\rho)_{min}$ = –3.128 e/Å^3 and $(\Delta/\sigma)_{max}$ = 0.000. The selected bond distances and bond angles are present in Table 1, while hydrogen bonds are given in Table 2.

Table 1. Selected Bond Lengths (Å) and Bond Angles (°)

Bond	Dist.	Bond	Dist.
Hg(1)–N(2)	2.16(2)	Hg(3)–Br(5)#1	2.424(2)
Hg(1)–N(2)#1	2.16(2)	Ho(1)–O(1)	2.325(15)
Hg(1)–Br(4)	2.788(3)	Ho(1)–O(2)#2	2.331(14)
Hg(1)–Br(4)#1	2.788(3)	Ho(1)–O(3)	2.308(19)
Hg(2)–Br(1)	2.493(4)	Ho(1)–O(4)#2	2.230(17)
Hg(2)–Br(2)	2.516(4)	Ho(1)–O(5)	2.381(14)
Hg(2)–Br(3)	2.663(3)	Ho(1)–O(6)#3	2.314(16)
Hg(2)–Br(4)	2.978(3)	Ho(1)–O(1W)	2.474(16)
Hg(3)–Br(5)	2.424(2)	Ho(1)–O(2W)	2.470(16)
Angle	(°)	Angle	(°)
N(2)#1–Hg(1)–N(2)	165.4(11)	Br(5)–Hg(3)–Br(5)#1	171.99(16)
N(2)#1–Hg(1)–Br(4)	95.1(6)	Hg(1)–Br(4)–Hg(2)	87.30(9)
N(2)–Hg(1)–Br(4)	94.5(5)	O(4)–Ho(1)–O(3)#2	96.3(7)
N(2)#1–Hg(1)–Br(4)#1	94.5(5)	O(4)–Ho(1)–O(6)#3	146.0(6)
N(2)–Hg(1)–Br(4)#1	95.1(6)	O(3)#2–Ho(1)–O(6)#3	81.1(6)
Br(4)–Hg(1)–Br(4)#1	97.89(13)	O(4)–Ho(1)–O(1)#3	139.1(6)
Br(1)–Hg(2)–Br(2)	131.49(14)	O(1)#3–Ho(1)–O(2W)	69.8(5)
Br(1)–Hg(2)–Br(3)	111.12(13)	O(4)–Ho(1)–O(2W)	70.0(5)
Br(2)–Hg(2)–Br(3)	109.69(12)	O(4)–Ho(1)–O(2)	81.5(6)
Br(1)–Hg(2)–Br(4)	99.73(12)	O(3)#2–Ho(1)–O(2)	144.4(6)
Br(2)–Hg(2)–Br(4)	99.06(13)	O(5)–Ho(1)–O(2W)	69.4(5)
Br(3)–Hg(2)–Br(4)	98.50(9)	O(1)#3–Ho(1)–O(2)	125.1(6)

Symmetry codes: #1: –*x*, *y*, –*z* + 1/2; #2: –*x* + 1, –*y*, –*z* + 1; #3: –*x* + 1, –*y* + 1, –*z* + 1

Table 2. Hydrogen Bonding Interactions

D–H ··A	D–H (Å)	H ··A (Å)	D ··A (Å)	D–H ··A (°)
N(1)–H(1B) ··O(7)#1	0.86	2.32	3.07(4)	175
N(3)–H(3A) ··O(8)#2	0.86	2.17	2.92(4)	146

Symmetry codes: #1: –*x*, 2 – *y*, 1 – *z*; #2: *x*, 2 – *y*, –1/2 + *z*

3 RESULTS AND DISCUSSION

The infrared spectrum shows that the peaks of complex **1** mainly reside in the frequency span of 400～1720 cm^{-1}. A very strong absorption peak at 3442 cm^{-1} can be ascribed to the ν_{O-H} stretching vibration of coordination water molecules. The weak absorption peak residing at 3079 cm^{-1} should come from the ν_{C-H} stretching vibration of pyridyl ring of the isonicotinic acid molecule. The very strong absorption peaks at 1621 and 1411 cm^{-1} can be attributed to the ν_{C-O} stretching vibration of coordinating carboxylic moieties, which suggests the coordination of all carboxylic moieties to metal ions. The absorption peak at 768 cm^{-1} should be due to the ν_{C-H} bending vibration of pyridyl ring.

Complex **1** was prepared from a reaction of $HgBr_2$, $Ho(NO_3)_3$ $6H_2O$, isonicotinic acid and distilled water via a hydrothermal reaction. Single-crystal X-ray diffraction analysis results show that **1** crystallizes in space group *P*2/*c* of monoclinic system with the *Z* value being two. The asymmetric unit of **1** consists of three crystallographically independent Hg^{2+} ions (Two of them are 0.5 occupancies), one Ho^{3+} ion, five bromide ions, one NO_3^- anion, three isonicotinic acid molecules and two coordination water molecules, as depicted in Fig. 2. Three Hg^{2+} ions locate in different coordination spheres. The Hg(1) ion has a four-coordinated tetrahedral conformation and is bound by two μ_2-bridging bromide ions and two nitrogen atoms of two isonicotinato ligands. The Hg(2) ion also shows a four-coordinated tetrahedral conformation and is surrounded by three terminal bromide ions and one μ_2-bridging bromide ion. Differently, the Hg(3) ion is only coordinated by two terminal bromide ions. The bond distance of Hg–N is 2.16(2) Å, while that of Hg–Br falls in the range of 2.424(2)～2.978(3) Å averaged by 2.634(4) Å. The bond distances for both Hg–N and Hg–Br are normal and comparable with those in the literature[42, 43]. The N–Hg–N bond angle is 165.4(11)°. The

N–Hg–Br bond angle falls in the range of 94.5(5)°~95.1(6)°, while that of Br–Hg–Br resides in the span of 97.89(13)°~171.99(16)°. The Hg(1)–Br(4)–Hg(2) bond angle is 87.30(9)°, close to a right-angle.

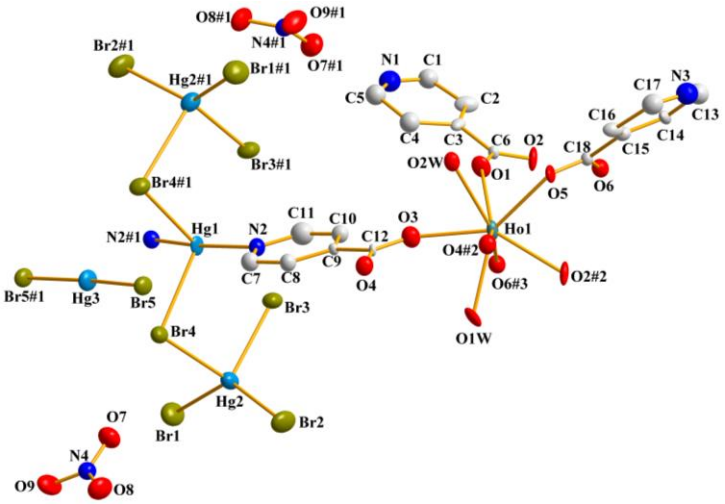

Fig. 2. An ORTEP view of compound 1 with hydrogen atoms being omitted for clarity. Displacement ellipsoids are drawn at the 20% probability level. Symmetry codes: #1: –*x*, *y*, –*z* + 1/2; #2: –*x* + 1, –*y*, –*z* + 1; #3: –*x* + 1, –*y* + 1, –*z* + 1

The Ho^{3+} ion displays a distorted square anti-prism conformation and is coordinated by six oxygen atoms from six isonicotinato ligands and two oxygen atoms of two coordination water molecules. The Ho(III)–O_{IA} bond distances in **1** fall in the span of 2.230(17)~2.381(14) Å with an average value of 2.314(19) Å, which is obviously shorter than that of Ho(III)–O_{water} (2.474(16) and 2.470(16) Å). This suggests that the Ho(III) ions have obviously stronger affinity to the isonicotinato ligands than to the water. All Ho(III)–O bond distances reside in the normal range and are comparable with that reported[44]. The O–Ho–O bond angles locate in the range of 69.4(5)°~146.0(6)°. The neighboring Ho(III) ions connect together via four or two isonicotinato ligands to yield a one-dimensional (1*D*) -Ho–$(IA)_4$–Ho–$(IA)_2$–Ho–$(IA)_4$–Ho–$(IA)_2$–Ho- chain running along the *b* direction, as presented in Fig. 3. The neighboring Ho(III)···Ho(III) distances are 4.3434(1) and 5.1335(2) Å in the chain. The 1*D* chains are interlinked by Hg(1) ions to give a two-dimensional (2*D*) layer parallel to the *bc* plane, as shown in Fig. 4. In complex **1**, all of the NO_3^- anions are isolated. As presented in Table 2, there are only two hydrogen bonding interactions existing in **1**, namely, N(1)–H(1B)···O(7) (–*x*, 2 – *y*, 1 – *z*) and N(3)–H(3A)···O(8) (*x*, 2 – *y*, –1/2 + *z*). Both of them just link the NO_3^- anions to the isonicotinato ligands, so they can not lead to a higher dimensional structure. With regard to complex **1**, the Van der Waals force, hydrogen bonding interactions and electrostatic interactions between the $[Ho(IA)(HIA)_2(H_2O)_2]^{2+}$ ions, $(Hg_3Br_8)^{2-}$ ions, $HgBr_2$ moieties and NO_3^- anions solidify the crystal packing structure (Fig. 5).

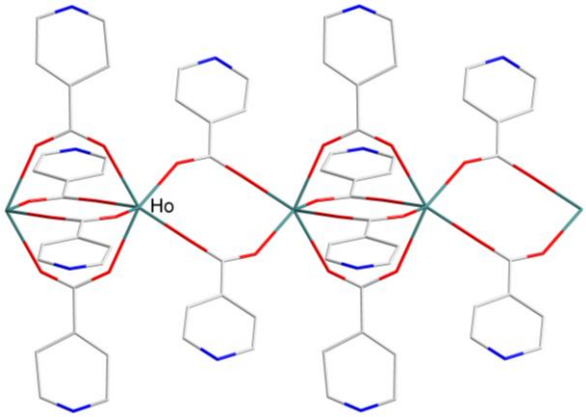

Fig. 3. A 1*D* -Ho–$(IA)_4$–Ho–$(IA)_2$–Ho–$(IA)_4$–Ho–$(IA)_2$–Ho- chain in compound 1

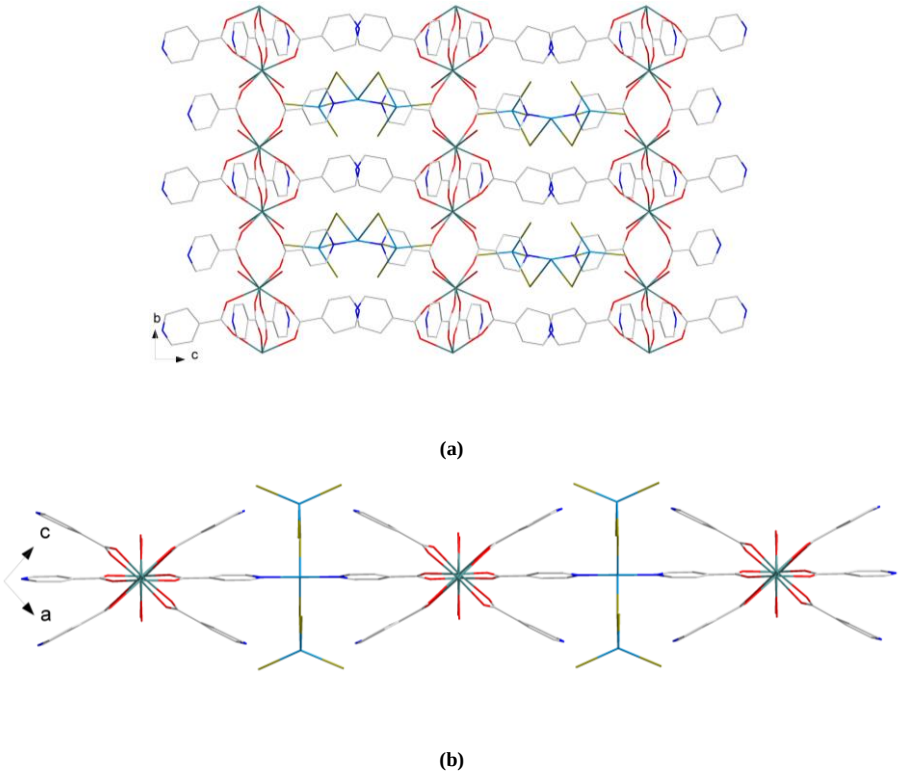

(a)

(b)

Fig. 4. A 2*D* layer viewed from different directions with directions *a* (a) and *b* (b)

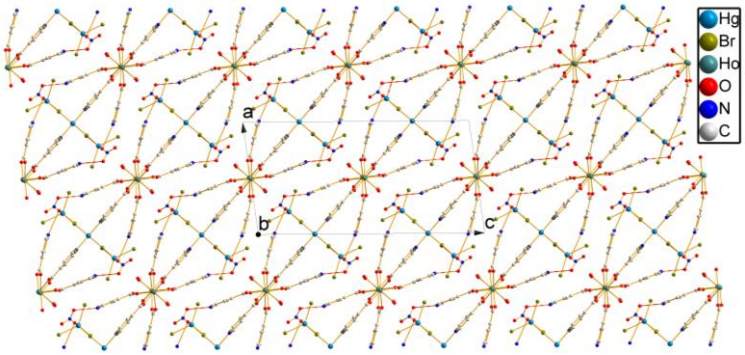

Fig. 5. A packing diagram of compound 1 with dashed lines representing the hydrogen bonding interactions (Å, °): N(1)–H(1B) ··O(7) (–*x*, 2 – *y*, 1 – *z*); N(3)–H(3A) ··O(8) (*x*, 2 – *y*, –1/2 + *z*)

It is well-known that holmium and mercury compounds can usually display photoluminescence. Therefore, the photoluminescence performance of the title compound was tested by using solid samples at room temperature. As given in Fig. 6, the photoluminescence adsorption of this compound locates in the range of 600～650 nm and the maximum peak is at 616 nm. When excited by the 616 nm wavelength, the compound shows two photoluminescence emission peaks that locate at 468 nm (blue region) and 545 nm (green region) and, the latter one is much stronger. These two emission peaks shall be attributed to the $^5I_8 \rightarrow {}^5G_6$ and $^5S_2 \rightarrow {}^5I_8$ characteristic emission of the 4*f* electron intrashell transition of the Ho(III) ions[45, 46]. With regard to complex **1**, it has a CIE chromaticity coordinate of (0.1774, 0.526) in the green region (Fig. 7). Therefore, **1** may be a potential green light emitting material. It should be pointed out that the excitation wavelength is 616 nm in the red region, but the emission wavelengths are in the blue and green regions. So, the photoluminescence of complex **1** is upconversion green emission.

Generally speaking, mercury materials can display semiconductor behaviors. For the sake of further investigating its photophysical performances, the solid state UV-visible diffuse reflectance spectrum of complex **1** was carried out at room temperature by using a powder sample. The solid state UV-visible diffuse reflectance spectrum data were converted with the Kubelka-Munk formula $\alpha/S = (1 - R)^2/2R$ that is

commonly applied for such research. With regard to this formula, α indicates the absorption coefficient, S is the scattering coefficient, while R stands for the reflection rate. With the use of linear epitaxy from the maximum absorption edge of the α/S versus energy curve, its semiconductive band gap value could be ascertained. As a result, by using this method, the semiconductive band gap of complex **1** is found to be 3.26 eV, as depicted in Fig. 8. From the diagram, several small bands smaller than 3.0 eV observed can be ascribed to the Ho(III) ions. Based on the band gap value of **1**, this complex may be a wide band gap semiconductive material. The maximum absorption edge of the diagram is not steep, so it shall undergo an indirect transition in this complex[47].

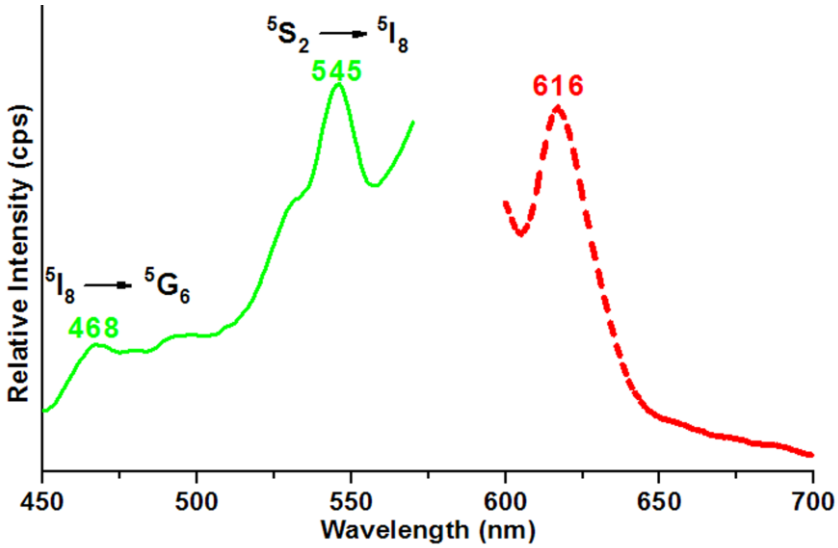

Fig. 6. Upconversion photoluminescence spectra of compound 1 measured using solid-state samples at room temperature with solid and dashed lines representing the emission and excitation spectra, respectively

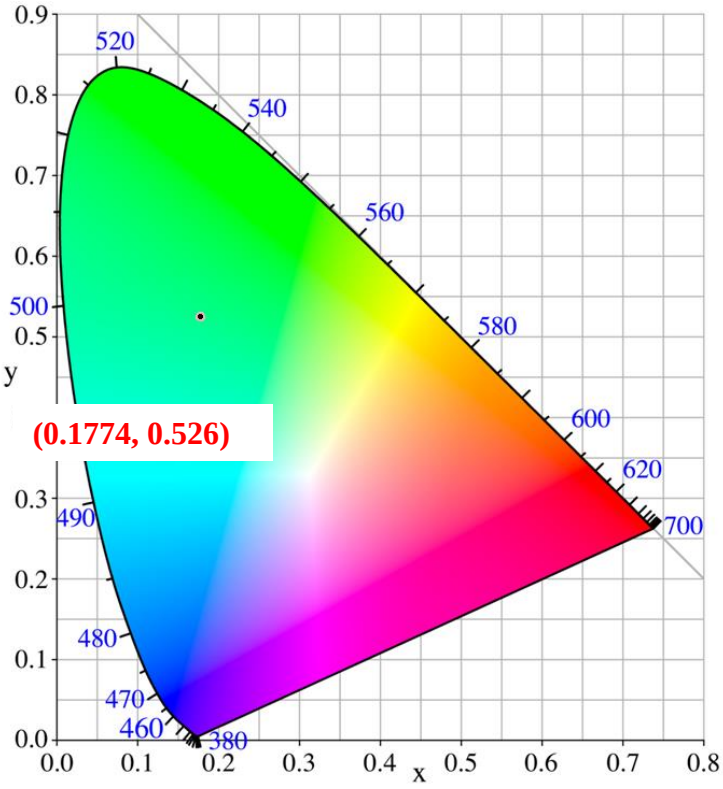

Fig. 7. A CIE chromaticity coordinate figure of 1

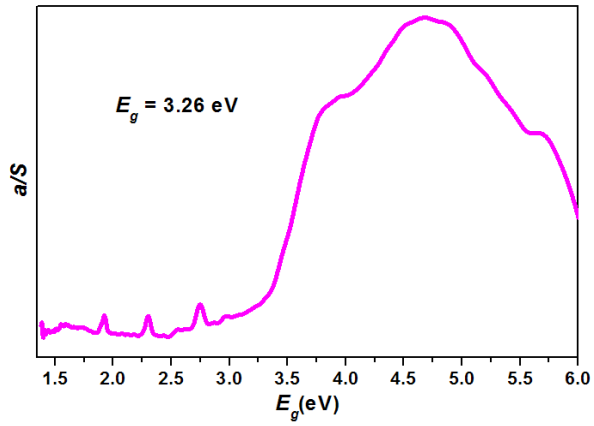

Fig. 8. A solid-state UV/Visible diffuse reflectance diagram of compound 1

The TG measurement of complex **1** was carried out under nitrogen atmosphere. As depicted in Fig. 9, complex **1** undergoes a four-step decomposition process with the weight loss being 4.10%, 28.17%, 43.09% and 12.15%, respectively. The total weight loss is 88.48%. On the first step (until 137 ℃) the weight loss is 4.10% due to the removal of all NO_3^- anions (calcd. 4.19%). In the second step from 137 to 240 ℃, the weight loss is 28.17% assigned to the departure of all isonicotinato ligands and water molecules (calcd. 28.21%). In the third step (from 240 to 480 ℃), the mass change is 43.09% probably due to the loss of Hg_3Br_8 moiety (calcd. 43.33%). The last step is from 480 to 700 ℃ with the weight loss of 12.15% caused by the removal of $HgBr_2$ moiety (calcd. 12.57%).

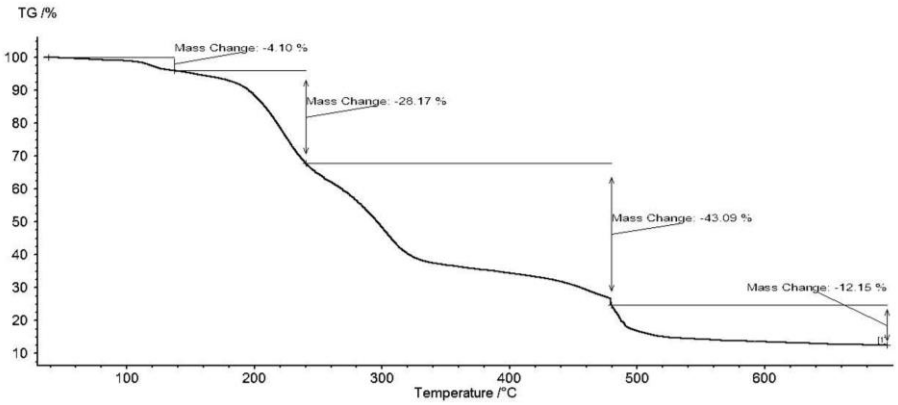

Fig. 9. TG curve of compound 1

A novel holmium-mercury compound was synthesized and characterized. This compound displays a two-dimensional layer-like structure. Using solid-state samples, it shows upconversion green photoluminescence emission. The emission peaks should be ascribed to the $^5I_8 \rightarrow {}^5G_6$ and $^5S_2 \rightarrow {}^5I_8$ characteristic emission of the 4*f* electrons of Ho^{3+} ions. This compound has a CIE chromaticity coordinate (0.1774, 0.526).

REFERENCES

(1) Wen, G. X.; Han, M. L.; Wu, X. Q.; Wu, Y. P.; Dong, W. W.; Zhao, J.; Li, D. S.; Ma, L. F. A multi-responsive luminescent sensor based on a super-stable sandwich-type terbium(III)-organic framework. *Dalton Trans*. **2016**, 45, 15492–15499.

(2) Liu, S. J.; Cao, C.; Xie, C. C.; Zheng, T. F.; Tong, X. L.; Liao, J. S.; Chen, J. L.; Wen, H. R.; Chang, Z.; Bu, X. H. Tricarboxylate-based Gd^{III} coordination polymers exhibiting large magnetocaloric effects. *Dalton Trans*. **2016**, 45, 9209–9215.

(3) Qiu, L. Y.; Yu, C. F.; Wang, X. L.; Xie, Y. B.; Kirillov, A. M.; Huang, W.; Li, J. P.; Gao, P.; Wu, T.; Gu, X. W.; Nie, Q.; Wu, D. Y. Tuning the solid-state white light emission of postsynthetic lanthanide-encapsulated double-layer MOFs for three-color luminescent thermometry applications. *Inorg.*

Chem. **2019**, 58, 4524–4533.

(4) Zhou, Z.; Gu, J. P.; Qiao, X. G.; Wu, H. X.; Fu, H. R.; Wang, L.; Li, H. Y.; Ma, L. F. Double protected lanthanide fluorescence core@shell colloidal hybrid for the selective and sensitive detection of ClO^-. *Sensor Actuat. B-Chem.* **2019**, 282, 437–442.

(5) Wei, J. H.; Yi, J. W.; Han, M. L.; Li, B.; Liu, S.; Wu, Y. P.; Ma, L. F.; Li, D. S. A water-stable terbium(III)-organic framework as a chemosensor for inorganic ions, nitro-containing compounds and antibiotics in aqueous solutions. *Chem. Asian J.* **2019**, 14, 3694–3701.

(6) Samannan, B.; Selvam, J.; Thavasikani, J. Synthesis, characterization and anticancer activity of transition metal substituted polyoxometalate-*β*-cyclodextrin composites. *Asian J. Chem.* **2020**, 32, 297–302.

(7) Xiong, X. H.; Tao, Y.; Yu, Z. W.; Yang, L. X.; Sun, L. J.; Fan, Y. L.; Luo, F. Selective extraction of thorium from uranium and rare earth elements using sulfonated covalent organic framework and its membrane derivate. *Chem. Engin. J.* **2020**, 384, 123240–7.

(8) Yao, X.; An, G. H.; Li, Y. X.; Yan, P. F.; Li, W. Z.; Li, G. M. Effect of nuclearity and symmetry on the single-molecule magnets behavior of seven-coordinated *β*-diketonate Dy(III) complexes. *J. Solid State Chem.* **2019**, 274, 295–302.

(9) Liu, S. J.; Cao, C.; Yao, S. L.; Zheng, T. F.; Wang, Z. X.; Liu, C.; Liao, J. S.; Chen, J. L.; Li, Y. W.; Wen, H. R. Temperature- and vapor-induced reversible single-crystal-to-single-crystal transformations of three 2*D*/3*D* Gd(III)-organic frameworks exhibiting significant magnetocaloric effects. *Dalton Trans.* **2017**, 46, 64–70.

(10) Ahmed, N.; Nisar, J.; Kouser, R.; Nabi, A. G.; Mukhtar, S.; Saeed, Y.; Nasim, M. H. Study of electronic, magnetic and optical properties of KMS_2 (M = Nd, Ho, Er and Lu): first principle calculations. *Mater. Res. Express* **2017**, 4, 065903–8.

(11) Wu, H. Q.; Yan, C. S.; Luo, F.; Krishna, R. Beyond crystal engineering: significant enhancement of C_2H_2/CO_2 separation by constructing composite material. *Inorg. Chem.* **2018**, 57, 3679–3682.

(12) Knoefel, N. D.; Schoo, C.; Seifert, T. P.; Roesky, P. W. A dimolybdenum paddlewheel as a building block for heteromultimetallic structures. *Dalton Trans.* **2020**, 49, 1513–1521.

(13) Li, J. Q.; Gong, L. L.; Feng, X. F.; Zhang, L.; Wu, H. Q.; Yan, C. S.; Xiong, Y. Y.; Gao, H. Y.; Luo, F. Direct extraction of U(VI) from alkaline solution and seawater via anion exchange by metal-organic framework. *Chem. Eng. J.* **2017**, 316, 154–159.

(14) Cai, H.; Li, N.; Zhang, N.; Yang, Z.; Cao, J.; Lin, Y.; Min, N.; Wang, J. Metal-directed supramolecular architectures based on the bifunctional ligand 2, 5-bis(1H-1,2,4-triazol-1-yl)terephthalic acid. *Acta Crystallogr. C* **2020**, 76, 118–124.

(15) Gong, L. L.; Feng, X. F.; Luo, F.; Yi, X. F.; Zheng, A. M. Removal and safe reuse of highly toxic allyl alcohol using a highly selective photo-sensitive metal-organic framework. *Green Chem.* **2016**, 18, 2047–2055.

(16) Zhao, Y.; Zhai, Z. M.; Liu, X. Y.; Yang, X. G.; Ma, L. F.; Wang, L. Y. Two cobalt(II) coordination polymers based on 5-i-butoxyisophthalate and dipyridyl: syntheses, structures and efficient oxygen evolution reaction. *J. Solid State Chem.* **2019**, 278, 120913–6.

(17) Anuja, K.; Reddy, K. H; Srinivasulu, K.; Dhanalakshmi, D. Synthesis, structural characterization and DNA binding studies on transition metal complexes with 2-formylpyridine benzoylhydrazone. *Asian J. Chem.* **2020**, 32, 322–328.

(18) Yin, W. H.; Xiong, Y. Y.; Wu, H. Q.; Tao, Y.; Yang, L. X.; Li, J. Q.; Tong, X. L.; Luo, F. Functionalizing a metal-organic framework by a photoassisted multicomponent postsynthetic modification approach showing highly effective Hg(II) removal. *Inorg. Chem.* **2018**, 57, 8722–8725.

(19) Martinez, B.; Livache, C.; Goubet, N.; Jagtap, A.; Cruguel, H.; Ouerghi, A.; Lacaze, E.; Silly, M. G.; Lhuillier, E. Probing charge carrier dynamics to unveil the role of surface ligands in HgTe narrow band gap nanocrystals. *J. Phys. Chem. C* **2018**, 122, 859–865.

(20) Fan, C. B.; Gong, L. L.; Huang, L.; Luo, F.; Krishna, R.; Yi, X. F.; Zheng, A. M.; Zhang, L.; Pu, S. Z.; Feng, X. F.; Luo, M. B.; Guo, G. C. Significant enhancement of C_2H_2/C_2H_4 separation by a photochromic diarylethene unit: a temperature- and light-responsive separation switch. *Angew. Chem. Int. Ed.* **2017**, 56, 7900–7906.

(21) Du, X.; Su, H.; Zhang, X. Metal-organic framework-derived M (M = Fe, Ni, Zn and Mo) doped Co_9S_8 nanoarrays as efficient electrocatalyst for water splitting: the combination of theoretical calculation and experiment. *J. Catal.* **2020**, 383, 103–116.

(22) Cheng, Y. J.; Wang, R.; Wang, S.; Xi, X. J.; Ma, L. F.; Zang, S. Q. Encapsulating $[Mo_3S_{13}]^{2-}$ clusters in cationic covalent organic frameworks: enhancing stability and recyclability by converting a homogeneous photocatalyst to a heterogeneous photocatalyst. *Chem. Commun.* **2018**, 54, 13563–13566.

(23) Wu, Y. P.; Tian, J. W.; Liu, S.; Li, B.; Zhao, J.; Ma, L. F.; Li, D. S.; Lan, Y. Q.; Bu, X. Bi-microporous metal-organic-frameworks with cubane $[M_4(OH)_4]$ (M = Ni, Co) clusters and pore space partition for electrocatalytic methanol oxidation reaction. *Angew. Chem. Int. Ed.* **2019**, 58, 12185–12189.

(24) Wu, X. X.; Fu, H. R.; Han, M. L.; Zhou, Z.; Ma, L. F. Tetraphenylethylene immobilized metal-organic frameworks: highly sensitive fluorescent sensor

for the detection of $Cr_2O_7^{2-}$ and nitroaromatic explosives. *Cryst. Growth Des.* **2017**, 17, 6041–6048.

(25) Liu, S. J.; Cao, C.; Yang, F.; Yu, M. H.; Yao, S. L.; Zheng, T. F.; He, W. W.; Zhao, H. X.; Hu, T. L.; Bu, X. H. High proton conduction in two Co^{II} and Mn^{II} anionic metal-organic frameworks derived from 1,3,5-benzenetricarboxylic acid. *Cryst. Growth Des*. **2016**, 16, 6776–6780.

(26) Yang, X. G.; Zhai, Z. M.; Lu, X. M.; Zhao, Y.; Chang, X. H.; Ma, L. F. Room temperature phosphorescence of Mn(II) and Zn(II) coordination polymers for photoelectron response applications. *Dalton Trans*. **2019**, 48, 10785–10789.

(27) Zhao, Y.; Deng, D. S.; Ma, L. F.; Ji, B. M.; Wang, L. Y. A new copper-based metal-organic framework as a promising heterogeneous catalyst for chemo- and regio-selective enamination of *β*-ketoesters. *Chem. Commun*. **2013**, 49, 10299–10301.

(28) Yang, X. G.; Ma, L. F.; Yan, D. P. Facile synthesis of 1*D* organic-inorganic perovskite micro-belts with high water stability for sensing and photonic applications. *Chem. Sci.* **2019**, 10, 4567–4572.

(29) Yao, S. L.; Liu, S. J.; Tian, X. M.; Zheng, T. F.; Cao, C.; Niu, C. Y.; Chen, Y. Q.; Chen, J. L.; Huang, H.; Wen, H. R. A Zn(II)-based metal-organic framework with a rare *tcj* topology as a turn-on fluorescent sensor for acetylacetone. *Inorg. Chem.* **2019**, 58, 3578–3581.

(30) Zhao, Y.; Wang, L.; Fan, N. N.; Han, M. L.; Yang, G. P.; Ma, L. F. Porous Zn(II)-based metal-organic frameworks decorated with carboxylate groups exhibiting high gas adsorption and separation of organic dyes. *Cryst. Growth Des.* **2018**, 18, 7114–7121.

(31) Luo, M. B.; Xiong, Y. Y.; Wu, H. Q.; Feng, X. F.; Li, J. Q.; Luo, F. The MOF^+ technique: a significant synergic effect enables high performance chromate removal. *Angew. Chem. Int. Ed*. **2017**, 56, 16376–16379.

(32) Fu, H. R.; Wang, N.; Qin, J. H.; Han, M. L.; Ma, L. F.; Wang, F. Spatial confinement of a cationic MOF: a SC-SC approach for high capacity Cr(VI)-oxyanion capture in aqueous solution. *Chem. Commun*. **2018**, 54, 11645–11648.

(33) Wang, H.; Meng, W.; Wu, J.; Ding, J.; Hou, H.; Fan, Y. Crystalline central-metal transformation in metal-organic frameworks. *Coor. Chem. Rev*. **2016**, 307, 130–146.

(34) Cryer, M. E.; Fiedler, H.; Halpert, J. E. Photo-electrosensitive memristor using oxygen doping in HgTe nanocrystal films. *ACS Appl. Mater. Inter*. **2018**, 10, 18927–18934.

(35) Fu, H. R.; Zhao, Y.; Zhou, Z.; Yang, X. G.; Ma, L. F. Neutral ligand TIPA-based two 2*D* metal-organic frameworks: ultrahigh selectivity of C_2H_2/CH_4 and efficient sensing and sorption of Cr(VI). *Dalton Trans.* **2018**, 47, 3725–3732.

(36) Yao, S. L.; Zheng, T. F.; Tian, X. M.; Liu, S. J.; Cao, C.; Zhu, Z. H.; Chen, Y. Q.; Chen, J. L.; Wen, H. R. Dicarboxylate-induced structural diversity of luminescent Zn^{II}/Cd^{II} coordination polymers derived from V-shaped bis-benzimidazole. *CrystEngComm.* **2018**, 20, 5822–5832.

(37) Zhai, Z. M.; Yang, X. G.; Yang, Z. T.; Lu, X. M.; Ma, L. F. Trinuclear Ni(II) oriented highly dense packing and *π*-conjugation degree of metal-organic framework for efficient water oxidation. *CrystEngComm.* **2019**, 21, 5862–5866.

(38) Zhao, Y.; Yang, X. G.; Lu, X. M.; Yang, C. D.; Fan, N. N.; Yang, Z. T.; Wang, L. Y.; Ma, L. F. $\{Zn_6\}$ Cluster based metal-organic framework with enhanced room-temperature phosphorescence and optoelectronic performances. *Inorg. Chem.* **2019**, 58, 6215–6221.

(39) Qin, J. H.; Huang, Y. D.; Zhao, Y.; Yang, X. G.; Li, F. F.; Wang, C.; Ma, L. F. Highly dense packing of chromophoric linkers achievable in a pyrene-based metal-organic framework for photoelectric response. *Inorg. Chem*. **2019**, 58, 15013–15016.

(40) Zhou, Z.; Han, M. L.; Fu, H. R.; Ma, L. F.; Luo, F.; Li, D. S. Engineering design toward exploring the functional group substitution in 1*D* channels of Zn-organic frameworks upon nitro explosives and antibiotics detection. *Dalton Trans.* **2018**, 47, 5359–5365.

(41) Sheldrick, G. M. Crystal structure refinement with SHELXL. *Acta Crystallogr. Sec. C-Struct. Chem*. **2015**, 71, 3–8.

(42) Lin, W. S.; Kuang, H. M.; Luo, H.; Chen, W. T. Upconversion photoluminescence and energy transfer mechanism of a novel terbium-mercury compound. *Chin. J. Struct. Chem.* **2019**, 38, 1012–1020.

(43) Lin, W. S.; Chen, W. T. Magnetic, photoluminescent and semiconductive properties of a novel 4*f*-5*d* bromide compound $(La_6Hg_5Br_{26})[4(HgBr_2)](2Br)$. *Chin. J. Struct. Chem.* **2020**, 1, 154–163.

(44) Kuang, H. M.; Zhang, Z. X.; Lin, L. Z.; Chen, H. L.; Chen, W. T. Preparation, structure, photoluminescence and energy transfer mechanism of a novel holmium complex. *Chin. J. Struct. Chem.* **2019**, 38, 337–344.

(45) Rajagopalan, K.; Jagannathan, T. Up/down conversion luminescence properties of $(Na_{0.5}Gd_{0.5})MoO_4:Ln^{3+}$ (Ln = Eu, Tb, Dy, Yb/Er, Yb/Tm, and Yb/Ho) microstructures: synthesis, morphology, structural and magnetic investigation. *New J. Chem.* **2014**, 38, 3480–3491.

(46) Tishchenko, M. A.; Gerasimenko, G. I.; Poluektov, N. S. Spectrophotometric study of the complexing of neodymium, holmium, and erbium ions with diantipyrylmethane and some of its homologs in aqueous-ethanol solutions. *Doklady Akademii Nauk SSSR* **1975**, 222, 1107–1110.

(47) Huang, F. Q.; Mitchell, K.; Ibers, J. A. New layered materials: syntheses, structures, and optical and magnetic properties of $CsGdZnSe_3$, $CsZrCuSe_3$, $CsUCuSe_3$, and $BaGdCuSe_3$. *Inorg. Chem.* **2001**, 40, 5123–5126.